Original Research

Specific Electrochemical Sensing of 4-Aminophenol Using a Graphene Oxide/Calcium Phosphate Nanocomposites Material for Pharmaceutical and Environmental Applications

Abdullah Asrar Ahamed [1], Narayanan Sudhan [2], Venkataraman Balasubramanian [3,*], Koyambo-Konzapa Stève-Jonathan [4,*], Viruthachalam Ramasamy Raja [5]

[1] Jamal Mohamed College (Autonomous), Affiliated to Bharathidasan University, Thiruchirapalli 620020, India;
[2] Thiagarajar College, Affiliated to Madurai Kamaraj University, Madurai 625009, India;
[3] Sona College of Technology, Affiliated to Anna University, Salem 636005, India;
[4] Laboratoire Matiere, Energie et Rayonnement (LAMER), University of Bangui, Bangui B.P. 1450, Central African Republic;
[5] Mannar Thirumalai Naicker College, Affiliated to Madurai Kamaraj University, Madurai 625004, India
* Correspondence: Venkataraman Balasubramanian, drvbsona@gmail.com; Koyambo-Konzapa Stève-Jonathan, koyamboj@yahoo.fr

Received: December 6, 2025; Accepted: February 3, 2026

Abstract: A graphene oxide-hydroxyapatite (GO/HA) nanocomposite was synthesized by a simple co-precipitation method and applied for the electrochemical determination of 4-aminophenol (4-AP). Structural, morphological, and functional group characterizations were carried out using X-ray diffraction, scanning electron microscopy, Fourier-transform infrared spectroscopy, and Raman spectroscopy. The electrochemical behavior of 4-AP at the GO/HA-modified glassy carbon electrode was investigated by cyclic voltammetry and differential pulse voltammetry. The modified electrode exhibited enhanced electron-transfer kinetics toward 4-AP, achieving a low detection limit of 0.14 nM and a wide linear concentration range of 0.1–340 μM with a correlation coefficient of $R_2 = 0.9974$. The high sensitivity is attributed to the synergistic effect of graphene oxide and porous hydroxyapatite within the nanocomposite. The proposed GO/HA-based sensing platform is rapid, simple, and sensitive, demonstrating potential applicability for the determination of 4-AP in pharmaceutical formulations and industrial wastewater samples.

Keywords: graphene oxide/hydroxyapatite nanocomposite; 4-aminophenol sensor; differential pulse voltammetry; pharmaceutical products

1. Introduction

Phenol and its derivatives are utilized extensively in the chemical industries and are thought to be extremely harmful to both humans and the environment when they are released into the environment. Aminophenol is one of the most harmful substances among them [1,2]. 4-aminophenol (C_6H_7NO) and its derivatives are frequently found in wastewater from the manufacturing of insecticides, herbicides, textile colours, paper, plastics, detergent, and cooking oil refineries. It can appear as a synthetic intermediate or breakdown product in pharmaceutical preparations of acetaminophen, which are highly harmful to aquatic life and give water an unpleasant taste [3]. 4-Aminophenol (4-AP) may subsequently enter the environment in large amounts as a pollutant that is highly harmful to human health because of its structural similarity to phenol and aniline. 4-AP targets the blood and kidneys in the body and is poisonous and irritating to the eyes, skin, and respiratory system [4]. Moreover, 4-AP has significant nephrotoxicity, teratogenicity, and potential

carcinogenicity, the European and US Pharmacopeia restrict its high levels in pharmaceuticals to 50 parts per million [5,6]. The majority of the sickness and deaths in drug poisoning cases are caused by overdosing on 4-AP. Hence, to determine 4-AP for the benefit of the environment and biomedicine, a straightforward, quick, and sensitive analytical technique must be developed. The presence of 4-AP has been ascertained using a few prominent detection methods, including spectrophotometry, liquid chromatography, and flow injection analysis [7–9]. Nevertheless, a number of these techniques are laborious, necessitate laborious sample preparation, and require costly equipment; they also present challenges when used to on-site studies. However, electrochemical sensors are appealing because of their quick reaction, excellent selectivity, affordability, ease of use, and ease of manufacture. As a graphene derivative, graphene oxide (GO) sheets have exceptional mechanical, thermal, and electrical properties, as well as quick electron transport and good biocompatibility. These attributes make them a good fit for potential uses in solar cells, energy storage capacitors, electrochemical sensors, and other fields [10–12]. Hydroxyapatite (HA) is a kind of calcium phosphate that chemically nearly matches with the main component of bone minerals. Which prop-up skeleton development by naturally building a layer of physiologically active apatite that mimics bone, due to its biocompatibility nature with several biological uses such as skeletal or dental implants and scaffolds for bone repair [13].

New functions like high electron mobility and exceptional catalytic activity are the result of graphene and HA working together. These nanohybrids are essential sorts of nanocomposite materials that efficiently mix the distinctive features of two material groups. Recent research has demonstrated that GO/HA nanocomposites are synthesizable and may find use in biological and bioactive domains [14,15].

In this research work, we show that GO/HA nanocomposites may be used to accurately measure 4-AP at pH 6.0 over a broad linear range of 0.1 μM to 340 μM. High sensitivity and good stability are demonstrated by the manufactured GO/HA modified GC electrode's outstanding electrocatalytic properties towards 4-AP.

2. Materials and Methods

2.1. Materials required

The analytical-grade reagents that were utilized didn't require any additional purification. We bought hydrogen peroxide (H_2O_2, 30% w/v solution), graphite, sulfuric acid, potassium permanganate, and 4-aminophenol from Sigma Aldrich. Merck provided the calcium nitrate tetrahydrate, cetyltrimethyl ammonium bromide, sodium phytate, and diammonium hydrogen orthophosphate. To prepare phosphate buffer solution by dissolving 0.1 M of each Na_2HPO_4 and NaH_2PO_4 in required amount of deionized water.

2.2. Instrumentations

A Bruker D8-ADVANCE diffractometer was used to perform powder X-ray diffraction (XRD) analyses using Cu Kα radiation with a wavelength of $\lambda = 0.15418$ nm. The samples' morphology was examined using a scanning electron microscope (SEM) (FEG QUANTA 250). Thermo Nicolect 380 Fourier Transform Infrared (FTIR) spectra were utilized for functional characterization studies. Raman spectra at room temperature were used to identify the functional groups of the GO/HA nanocomposite. CHI electrochemical workstation (model CHI660E) were used to perform electrochemical experiments. The working electrode was a 3 mm glassy carbon (GC), the reference electrode was Ag/AgCl (saturated KCl), and the auxiliary electrode was a Pt wire. Using 0.1 M PBS (pH 6.0) containing 100 μM 4-AP, cyclic voltammograms (CVs) were collected at a scan rate of 50 mV/s within a potential window of −0.2 V to 0.5 V. By scanning potential between −0.2 V and 0.6 V with amplitude of 20 mV and a pulse width of 5 mV, differential pulse voltammograms (DPVs) were produced.

2.3. Synthesis of graphene oxide (GO)

A modified version of Hummer's technique was used to prepare the graphene oxide (GO) [16]. In short, 50 mL of strong sulfuric acid that had been chilled by an ice water bath was mixed with 1 g of graphite. After that, 4 g of $KMnO_4$ were slowly added, and then the mixture was allowed to magnetic stirring for one hour. Subsequently, 200 mL of H_2O were mix with the above solution and it was continuously allowed to stirring for half hour. 3 millilitres of 30% H_2O_2 were gradually added, while observing the solution colour from deep brown to green. Centrifugation was used to extract the solid graphite oxide, which was then repeatedly cleaned with deionized water and vacuum dried.

2.4. Synthesis of the GO/HA composite

The GO/HA nanocomposite was created using a straightforward co-precipitation process [17]. In short, 1 mL of deionized water was used to dissolve 2 milligrams of dried GO. Then, 94 mg of $Ca(NO_3)$ (40 weight percent). A colloidal suspension was created by adding H_2O to 90 mL of GO colloid solution and ultrasonically treating it for 60 min. To create solution A, 25 mg of CTAB was then added to the mixture and sonicated for 60 min. Solution B was created by adding 18.23 mg of $(NH_4)_2HPO_4$ and almost a gram of sodium phytate to 15 mL of ultrapure water. This solution was then added to solution A. After 30 min of sonication, the combined solution was maintained for 12 h at 180 °C in a hot air oven. After repeatedly washing the composite with ethanol and water to get rid of the sodium phytate and CTAB ions, the finished product was dried for 24 h at 60 °C. CTAB was employed as a surfactant and structure-directing agent to improve the dispersion of GO sheets and promote uniform nucleation of HA nanoparticles on the GO surface. Sodium phytate acted as a chelating phosphate source, enabling controlled HA crystal growth and enhancing the stability and homogeneity of the GO/HA nanocomposite.

2.5. Preparation of real samples

Commercial paracetamol tablets were accurately weighed and finely ground using a mortar and pestle. The resulting powder was dispersed in 100 mL of deionized water, sonicated for 30 min to obtain a homogeneous solution, and subsequently filtered through Whatman filter paper to remove insoluble excipients. The filtrate was then appropriately diluted with phosphate buffer solution (PBS, pH 6.0) to prepare the required concentrations for electrochemical measurements.

2.6. Electrode preparation method

The working electrode was carefully polished with 0.5 μm alumina slurry using an alumina cloth to remove physically adsorbed particles. Five milligrams of GO/HA composite were dispersed in 1 mL of deionized water using an ultrasonicator. Subsequently, 10 μL of the resulting suspension was drop-cast onto the surface of the GCE and allowed to dry at room temperature to obtain the GO/HA-modified GCE.

3. Result and Discussion

3.1. Analyzing structural formation

The powder X-ray diffraction (XRD) patterns of graphene oxide (GO), pristine hydroxyapatite (HA), and the graphene oxide-hydroxyapatite nanocomposite (GO/HA) are presented in Figure 1(A). The XRD pattern of pristine GO exhibits a characteristic diffraction peak corresponding to the (001) plane, indicating the presence of oxygen-containing functional groups and an expanded interlayer spacing [18]. In contrast, the GO/HA composite displays a prominent diffraction peak centered at $2\theta \approx 22°$, which is attributed to the partial reduction of GO to graphene during the composite formation process, consistent with earlier reports [8]. The disappearance of the GO (001) peak further supports the effective reduction and exfoliation of GO sheets within the nanocomposite matrix. The successful incorporation of hydroxyapatite onto the graphene oxide framework is confirmed by the presence of

well-defined diffraction peaks in the GO/HA composite corresponding to the (002), (211), (213) and (222) planes of crystalline HA. These peaks are in good agreement with the standard diffraction data of hexagonal hydroxyapatite (ICDD/JCPDS card No. 09–0432), indicating the preservation of the HA crystal structure upon composite formation. No additional impurity peaks are observed, suggesting the high phase purity of the synthesized materials. The calculated crystallite sizes were approximately 22.8 nm for pristine HA and 73 nm for the GO/HA nanocomposite. The notable increase in crystallite size for the GO/HA composite can be attributed to the effective nucleation and growth of HA crystals on the graphene oxide surface, facilitated by strong interfacial interactions and the high surface area of graphene oxide sheets. These structural features are expected to enhance the physicochemical properties of the composite, making it promising for advanced functional sensor applications.

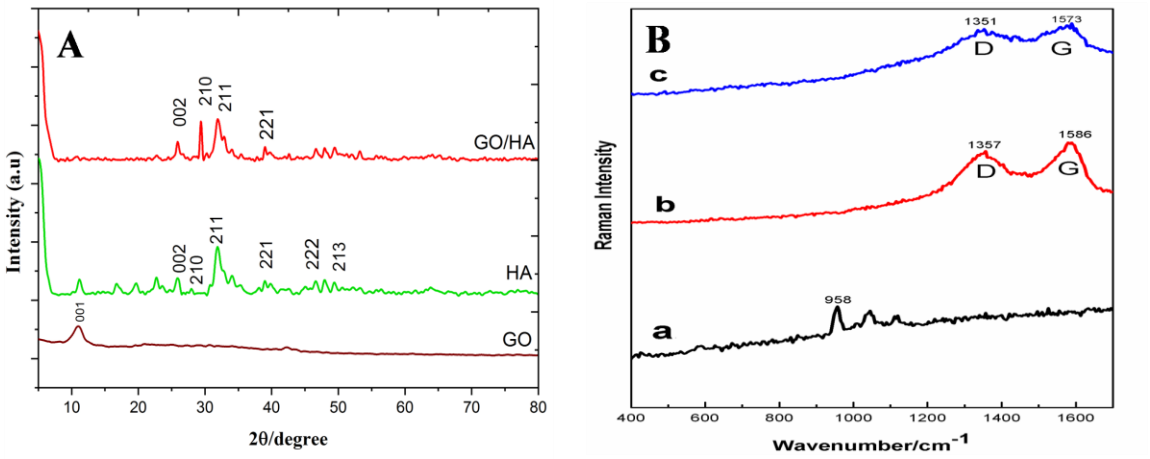

(A) (B)

Figure 1. (A) X-ray diffraction patterns of GO, HA, and GO/HA nanocomposite; (B) Raman spectra of a) HA, b) GO, c) GO/HA.

Raman spectroscopy was employed to confirm the formation of GO, HA, and the GO/HA composite. The characteristic symmetric stretching vibration of phosphate groups in hydroxyapatite appears at ~958 cm^{-1} (Figure 1(Ba)). The Raman spectrum of GO shows the typical D band at 1357 cm^{-1}, associated with structural defects, and the G band at 1586 cm^{-1}, corresponding to the in-plane vibration of sp^2-hybridized carbon atoms (Figure 1(Bb)). In the GO/HA composite (Figure 1(Bc)), the D and G bands are downshifted to 1351 cm^{-1} and 1573 cm^{-1}, respectively. The I_D/I_G ratio increases from 0.91 (GO) to 0.97 (GO/HA), indicating an increase in defect density due to interfacial interactions between GO and HA, confirming successful composite formation [9].

3.2. FT-IR analysis

The FTIR spectra of HA, GO, and the GO/HA composite (Figure 2) exhibit broad absorption bands in the range of 3446–1633 cm^{-1}, which are attributed to adsorbed water molecules, while the peak at 3567 cm^{-1} corresponds to O–H stretching vibrations. In GO, characteristic bands at 1089 cm^{-1} (C–O stretching), 1384 cm^{-1} (C–O–H deformation), 1615 cm^{-1} (C = C stretching), and 1730 cm^{-1} (C = O stretching of the COOH group) confirm the presence of oxygen-containing functional groups, particularly epoxide groups on the basal plane of graphene. Upon reduction, the broad absorption associated with these oxygenated functional groups markedly diminishes or disappears, indicating effective reduction of GO. The emergence of a peak at 1566 cm^{-1} is assigned to the skeletal vibrations of reduced graphene sheets [10]. Furthermore, the characteristic phosphate (PO_4^{3-}) vibrations of HA are observed at 562, 603, and 1032 cm^{-1}. Collectively, these spectral features confirm the successful formation and integration of GO and HA in the composite material.

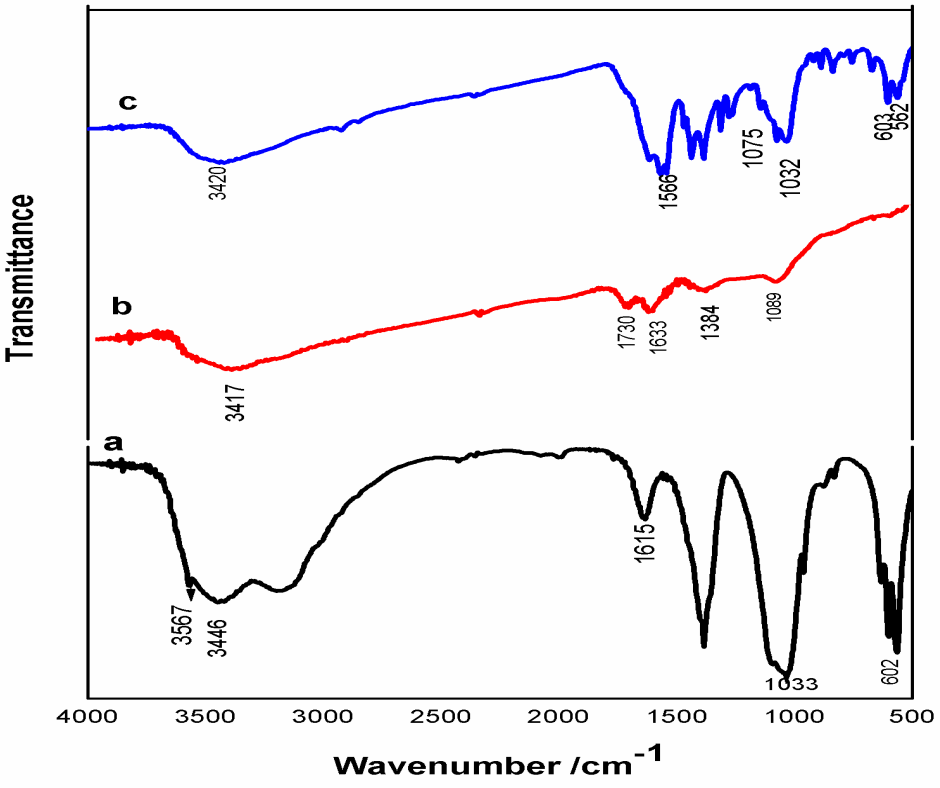

Figure 2. FT-IR spectra of (a) HA; (b) GO; (c) GO/HA.

3.3. Surface morphological studies

FESEM were used to observe both the morphological characteristics of GO, HA, and GO/HA. A SEM picture of HA nanoparticles is displayed in Figure 3(Aa). As seen from these images, there was a flake of hydroxyapatite nanoparticles develop perpendicularly. Figure 3(Ab) illustrates that the SEM images of GO sheets. The uniform aggregation of HA nanoparticles on graphene sheets with a restricted size distribution is shown in Figure 3(Ac). On the GO surface, the HA nanoparticles were uniformly anchored. The restacking of graphene sheets is reduced by the uniform dispersion of HA nanoparticles. In Figure 3(B) shows the EDAX analysis of conformation of hydroxyapatite nanoporous are comprised by Ca/P in GO/HA samples.

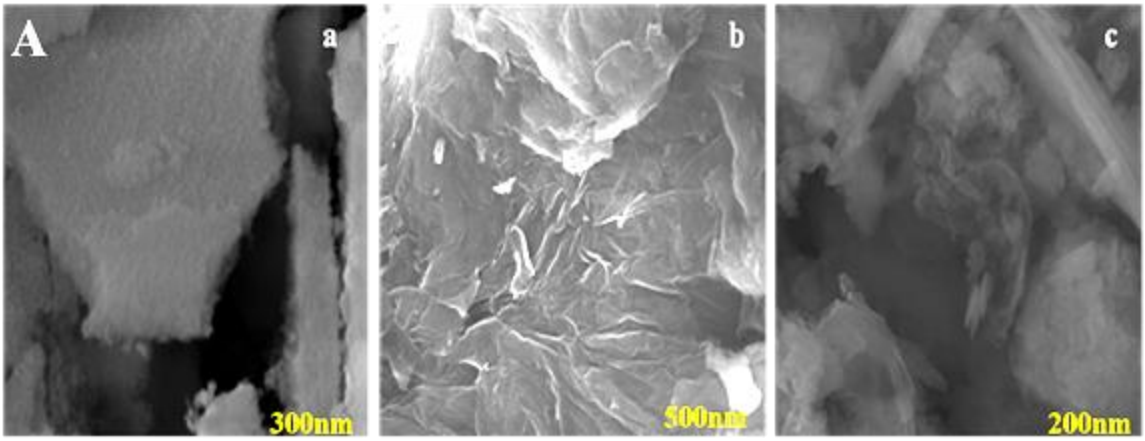

(**A**)

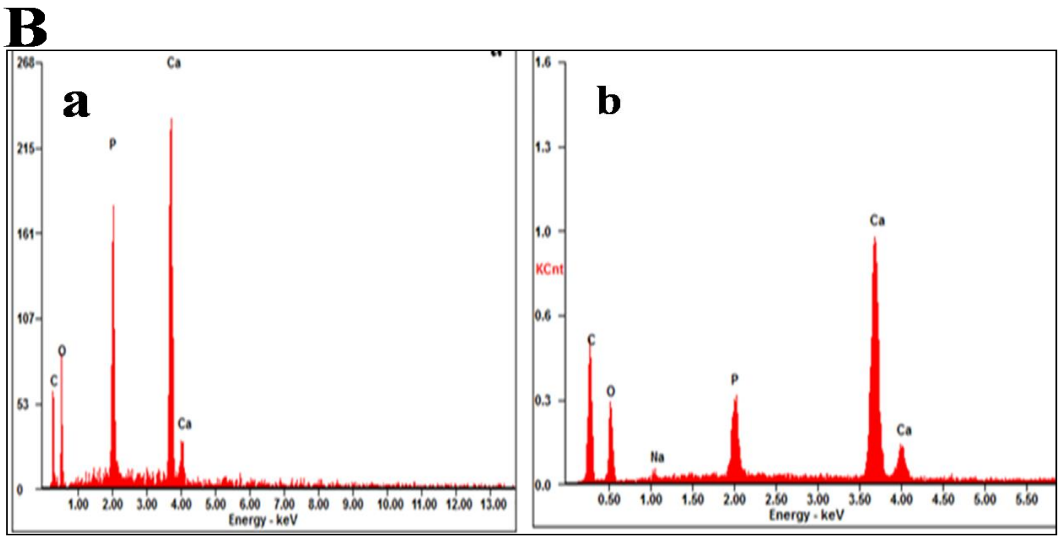

(B)

Figure 3. (A) SEM image of a) Pure HA, b) Pure GO, c) GO/HA; (B) EDAX analysis of Pure a) HA and b) GO/HA.

3.4. Electrochemical characterization of 4-aminophenol

CV was used to analyze the electrochemical behaviour of 4-AP at various modified electrode surface such as unmodified GCE (curve a), GO/GCE (curve b), HA/GCE (curve c), and GO/HA/GCE (curve d) in PBS (pH 6.0) at the fixed scan rate of 50 mV/s are shown in Figure 4(A). Significantly, a little, distinct redox wave was visible at the exposed electrode (curve a). The oxidation peak current (9.5 μA) at the GO/HA nanocomposite (curve d) modified GCE was two times greater than that at the HAP (3.2 μA) and GO (3.9 μA) modified GCE. In addition to increasing the redox peak currents, the modified GO/HA/GCE also increases the reversibility of the 4-AP redox reaction. This can mainly be attributed to the large surface area and subtle electronic properties of graphene oxide serves as an efficient electron transport matrix due to its two-dimensional conductive network. Although, GO is intrinsically less conductive than pristine graphene, its practical reduction during composite formation significantly improves conductivity. The intimate contact between GO and HA facilates rapid electron transfer from the analyte-binging sites on HA to the electrode interface surface via GO sheets. Figure 4(B) displays the CVs of the GO/HA nanocomposite coated GC electrode in PBS (pH 6.0) with and without addition of 4-AP. Without 4-AP, it is clear that there is no redox peak (curve a). Curve b shows that when 4-AP was added to PBS, two well-redox peaks with a peak-to-peak separation (ΔEP) of 45 mV were observed. This suggests that the performance of the electrode with increased electrocatalytic activity towards 4-AP has been significantly enhanced by the GO/HA nanocomposite.

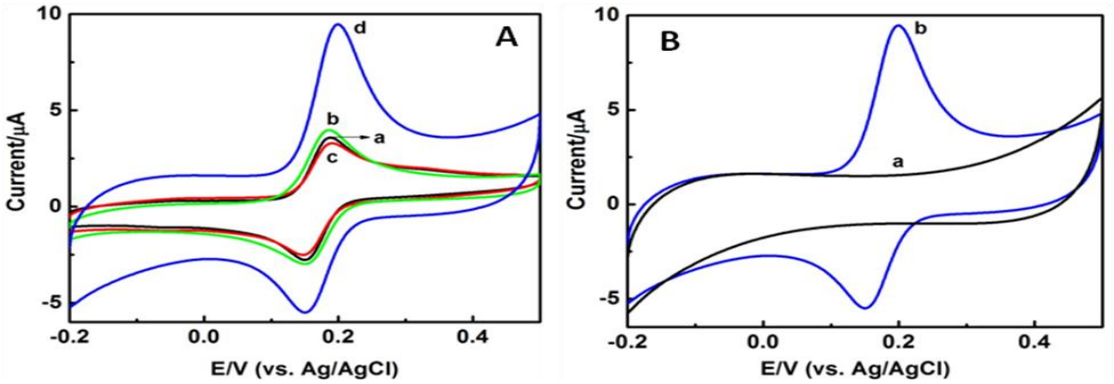

Figure 4. (A) CVs for 4-AP (75 μM) at the (a) bare GCE, (b) GO/GCE, (c) pristine HA/GCE and (d) GO/HA/GCE recorded in PBS (pH 6.0) solution at a fixed scan rate of 50 mV/s in the potential between −0.2 V and 0.5 V; (B) CVs obtained at GO/HA/GCE (a) in the absence and (b) presence 4-AP (75 μM) in 0.1 M PBS (pH 6.0).

3.5. Optimization of electrochemical characteristics of the GO/HA-modified glassy carbon electrode

3.5.1. Effect of scan rate

The influence of scan rate on the redox behavior of 4-aminophenol (4-AP) was investigated at the GO/HA-modified glassy carbon electrode in 0.1 M phosphate buffer solution (pH 6.0). As shown in Figure 5(A), both anodic and cathodic peak currents increase linearly with increasing scan rate in the range of 50–500 mV s^{-1}. The corresponding linear relationships between scan rate and peak currents (inset of Figure 5(A)) indicate that the electrochemical process of 4-AP at the GO/HA/GCE is governed by a surface-controlled mechanism. With increasing scan rate, the anodic peak potential (E_{pa}) shifts toward more positive values, while the cathodic peak potential (E_{pc}) shifts toward more negative values, suggesting quasi-reversible electron transfer kinetics. Furthermore, the redox reaction of 4-AP at the GO/HA nanocomposite-modified electrode involves a two-electron and two-proton transfer process, consistent with the electrochemical oxidation of 4-AP to its corresponding quinone-imine species. The enhanced electrochemical performance can be attributed to the synergistic interaction between graphene oxide and hydroxyapatite, which facilitates efficient charge transfer and promotes strong adsorption of 4-AP on the electrode surface as represented in the Scheme 1. The surface-controlled behaviour is further supported by the linear dependence of peak current on scan rate rather than on the square root of scan rate.

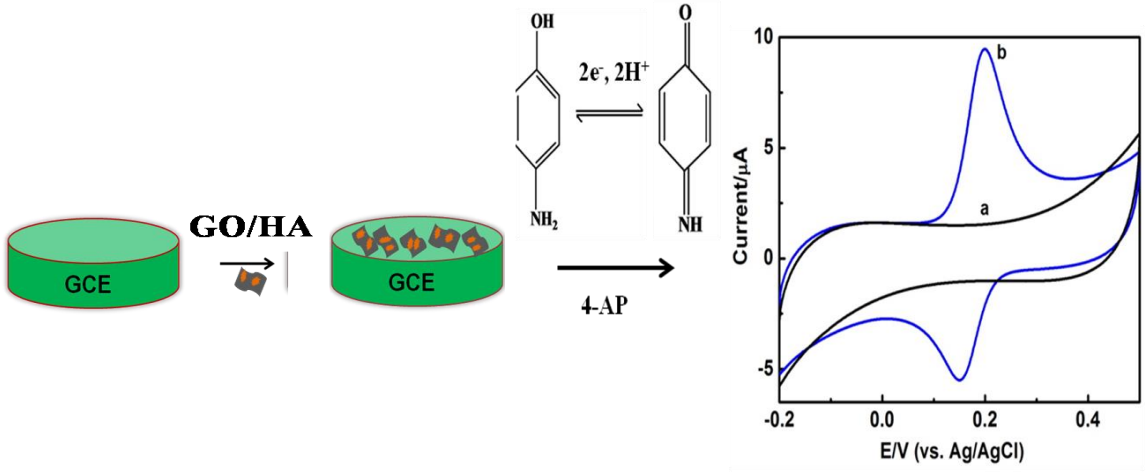

Scheme 1. 4-aminophenol detection scheme using GO/HA/GCE.

3.5.2. Effect of pH

The effect of pH on the electrochemical behavior of 4-aminophenol (4-AP, 100 μM) at the GO/HA nanocomposite-modified glassy carbon electrode was investigated by cyclic voltammetry in phosphate buffer solution over the pH range of 4.0–9.0 at a scan rate of 50 mV s^{-1}. The oxidation peak current increases with increasing pH from 4.0 to 6.0 and decreases at higher pH values, with the maximum current response observed at pH 6.0. At this pH, the GO/HA/GCE exhibits enhanced electrocatalytic activity toward 4-AP, yielding a maximum oxidation peak current of 9.5×10^{-6} A. Accordingly, pH 6.0 phosphate buffer was selected as the optimum medium for subsequent electrochemical sensing of 4-AP. The enhanced response at pH 6.0 can be attributed to the optimal proton availability for the proton-coupled electron transfer process of 4-AP, along with favourable adsorption of 4-AP on the GO/HA surface, which together promote efficient electro-catalytic oxidation. 4-AP exists predominantly in a neutral or weakly protonated form which enhances π–π interactions and hydrogen bonding with GO sheets and HA surface sites, improving surface adsorption and electron transfer. At higher pH values, partial deprotonation reduces adsorption efficiency, leading to lower current.

3.5.3. Electro catalytic behaviour of GO/HA/GCE in 4-aminophenol

Figure 5(B) shows the linear sweep voltammograms (LSVs) recorded for 4-AP at the GO/HA-modified electrode over a concentration range of 0–100 μM. With successive additions of 10 μM 4-AP, the oxidation peak current increases proportionally, accompanied by a slight negative shift in the oxidation peak potential. A good linear relationship between oxidation peak current and 4-AP concentration is obtained, with a correlation coefficient (R^2) of 0.997 (inset of Figure 5(B)), demonstrating the suitability of the GO/HA/GCE for the quantitative electrochemical determination of 4-AP.

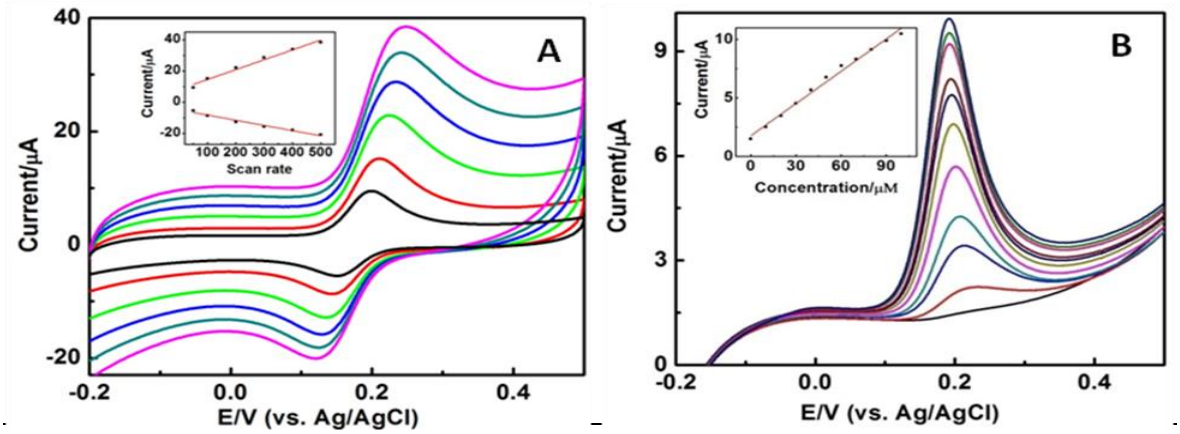

Figure 5. (A) CVs of GO/HA/GCE in 4-AP (100 μM) at different scan rates: 50–500 mV/s. Inset: plot of anodic and cathodic peak current vs. scan rate and (B) LSVs obtained for 4-AP from the range 0 to 100 μM.

3.5.4. Analytical performance of 4-aminophenol using GO/HA/GCE

Differential pulse voltammetry (DPV) was employed to evaluate the linear range and limit of detection (LOD) of 4-aminophenol (4-AP), owing to its significantly higher current sensitivity compared to cyclic voltammetry. Figure 6 shows the DPV responses of the GO/HA modified GCE recorded at different concentrations of 4-AP in 0.1 M PBS (pH 6.0) that thescanning potential between −0.2 V and 0.6 V with amplitude of 20 mV and a pulse width of 5 mV. A well-defined and proportional increase in the oxidation peak current was observed with increasing 4-AP concentration. The corresponding calibration curve exhibited a good linear relationship between peak current and 4-AP concentration over the range of 0.1–340 μM, with a correlation coefficient of $R^2 = 0.9974$, indicating

excellent linearity. The limit of detection (LOD) was calculated using the standard equation: LOD = $3\sigma/S$ where σ represents the standard deviation of the blank signal (n = 10) and S is the slope of the calibration curve. Based on this calculation, the LOD for 4-AP was determined to be 0.14 nM, demonstrating the high sensitivity of the GO/HA modified electrode. (Table 1. Ref. [19–24]) compares the analytical performance of the GO/HA modified GCE with other recently reported modified electrodes for 4-AP detection. It is evident that the present sensor exhibits a wide linear dynamic range and one of the lowest detection limits among the reported systems [19–24]. Notably, the detection limit achieved with the GO/HA modified GCE is significantly lower than those reported for graphene-chitosan composite modified electrodes, paper-based microfluidic devices, and hemin-based molecularly imprinted polymer (MIP) grafted GCEs [19–21].

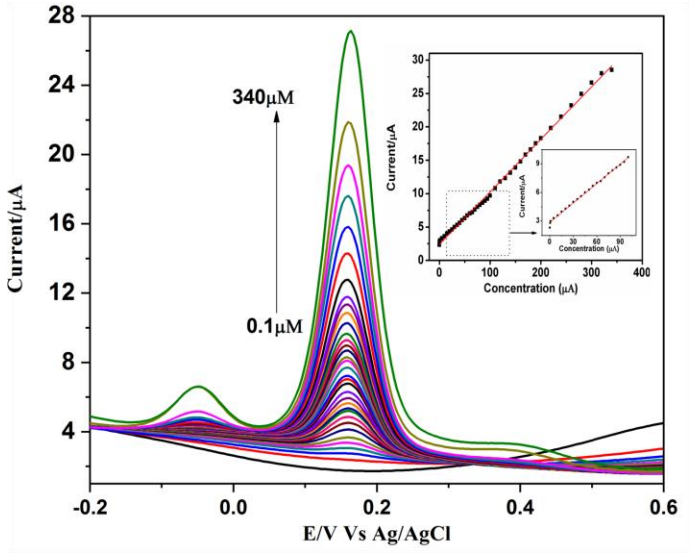

Figure 6. Voltammetric response of the GO/HA-modified glassy carbon electrode toward different concentrations of 4-aminophenol (4-AP) under optimized conditions scanning potential between −0.2 V and 0.6 V with amplitude of 20 mV and a pulse width of 5 mV in 0.1 M phosphate buffer solution at (PBS, pH 6.0) Figure 6. Inset shows the corresponding calibration plots of DPV response towards 4-AP.

Table 1. Comparison of the responses of other 4-aminophenol sensor.

Electrodes	Technique	Linear range (μM)	Detection limit (μM)	Reference
[a]MIP	Amp	10–90	3	[19]
[b]Graphene-chitosan	DPV	0.2–550	0.057	[20]
[c]GR/PANI	DPV	0.2–100	0.0065	[21]
Paper based microfludic device	Amp	0.05–2.0	10	[22]
[d]MPA/SAM/AU	SWV	0.04–8	0.012	[23]
[e]SWNT/nafion	AdSV	0.005–2.0	0.0008	[24]
[f]GO/HA nanocomposite	DPV	0.1–340	0.014	Presentwork

[a] hemin based molecular imprinted polymer modified glassy carbon electrode (GCE); [b] graphene-chitosan modified GCE; [c] graphene-polyaniline modified GCE; [d] mercaptopropionic acid (MIP) modified Au electrode; [e] single walled nanotube/nafion modified GCE; [f] graphene-cxide-hydroxyapatite modified GCE.

3.6. Selectivity studies

As shown in the Figure 7, the addition of a 100-fold excess of common interfering species, such as NaCl, $MgCl_2$, L-tyrosine, glucose, as well as structurally related compounds (2-AP and 3-AP), produced no significant change in the current response. In contrast, each addition of 4-AP resulted in a distinct and sharp increase in the oxidation current, indicating a highly selective response of the sensor toward 4-AP. The negligible variation in current in the presence of interfering species confirms that these substances do not participate in the electrochemical reaction at the applied potential. This excellent selectivity can be attributed to the preferential adsorption and faster electron-transfer kinetics of 4-AP at the GO/HA modified electrode surface. Overall, these results demonstrate that the fabricated electrode is highly suitable for the selective determination of 4-aminophenol, even in the presence of a large excess of electroactive and structurally similar interfering compounds.

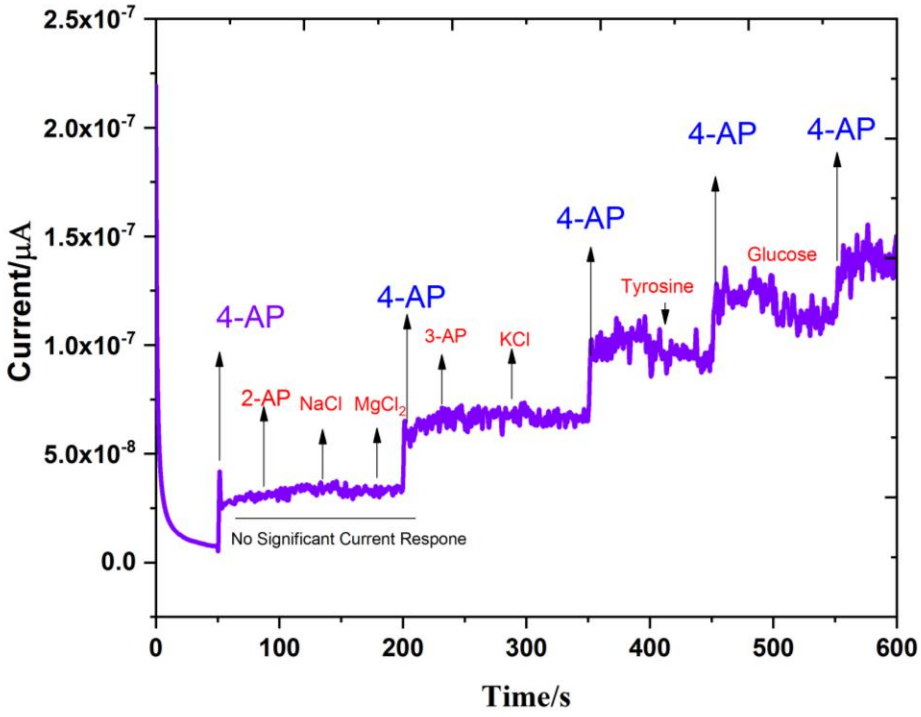

Figure 7. Amperometric responses of the GO/HA-modified electrode toward 4-AP in the presence of common interfering species (NaCl, $MgCl_2$, KCl, tyrosine, and glucose) in PBS (pH 6.0).

At 100 μM 4-aminophenol, five successive voltametric measurements yielded a %RSD of 4.7%, which is acceptable for phenolic analytes at high concentrations and can be attributed to mild adsorption of oxidation products, as reported in earlier electrochemical studies. The stability of the proposed sensor was investigated. After 20 cyclic runs, while the naked GCE shows over 17.14% loss from the starting value, the voltammetric response of GO/HA/GCE only revealed 2.71% loss. According to these findings, the GO/HA modified electrode exhibits good stability and repeatability.

3.7. Method validation according to ICH guidelines

The analytical performance of the proposed GO/HA-modified glassy carbon electrode for the determination of 4-aminophenol (4-AP) was validated in accordance with the International Council for Harmonisation (ICH) guidelines (Q2(R1)). Validation parameters including linearity, accuracy, precision, sensitivity (LOD and LOQ), recovery, and statistical comparison with a reported method were systematically evaluated to confirm the reliability and applicability of the developed electrochemical method.

3.7.1. Regression parameters, linearity, precision, LOD and LOQ

Linearity of the proposed method was evaluated by differential pulse voltammetry under optimized conditions over the concentration range of 0.1–340 μM of 4-AP. A strong linear relationship between oxidation peak current and analyte concentration was obtained, with a correlation coefficient (R^2) of 0.9974, confirming excellent linearity.

The sensitivity of the method was assessed by calculating the limit of detection (LOD) and limit of quantification (LOQ) using the equations LOD = 3σ/S and LOQ = 10σ/S, where σ is the standard deviation of the blank signal (n = 10) and S is the slope of the calibration curve. The low LOD and LOQ values demonstrate the high sensitivity of the GO/HA-modified electrode.The analytical performance parameters of the fabricated sensor, including linear range, correlation coefficient, LOD, and LOQ, are summarized in Table 2.

Accuracy was evaluated through recovery studies, while precision was assessed in terms of repeatability (intra-day precision) and expressed as percentage relative standard deviation (%RSD). The obtained %RSD values were within acceptable limits as per ICH guidelines, indicating good method precision and reproducibility.

Table 2. Regression Parameters of the Proposed Electrochemical Method.

Parameters	Value
Linear Range (μM)	0.1–340
Regression Equation	Ip (μA) = ax + b
Correlation coefficient (R^2)	0.9974
Limit of Detection (LOD, nM)	0.14
Limit of Quantification (LOQ, nM)	0.47 (10σ/S)
Precision (%RSD, n = 5)	≤ 4.7

3.7.2. Statistical comparison with reported method

The accuracy and precision of the proposed GO/HA-modified electrode were statistically compared with a previously reported electrochemical method for 4-AP determination using Student's *t*-test and *F*-test at a 95% confidence level (p = 0.05). The calculated t and F values were found to be lower than the corresponding theoretical values, indicating that there is no statistically significant difference between the proposed and reported methods in terms of accuracy and precision.

These results confirm the validity, robustness, and reliability of the developed electrochemical sensing method.

3.7.3. Validation of 4-AP by standard addition technique in real pharmaceutical samples

To evaluate the applicability of the proposed sensor for real sample analysis, the GO/HA-modified electrode was employed for the determination of 4-AP in pharmaceutical formulations. Commercial tablets were finely ground, dissolved in deionized water, sonicated, and filtered to remove insoluble excipients. The resulting solution was appropriately diluted with phosphate buffer solution (pH 6.0) prior to analysis. Spiked recovery experiments were carried out by adding known concentrations of 4-AP to the pretreated samples. Satisfactory recovery values were obtained, demonstrating the accuracy and reliability of the proposed sensor for the determination of 4-AP in real pharmaceutical samples. The results obtained for the determination of 4-AP in pharmaceutical formulations using the GO/HA/GCE sensor are summarized in Table 3. While environmental sample

analysis was not performed in the current work, recent literature illustrates successful application of electrochemical sensors to real matrices with greenness assessment [24,25]. This underscores the feasibility of extending the present GO/HA sensor to wastewater and agricultural samples in future studies, with proper matrix treatment and sustainability evaluation.

Table 3. Detection of 4-AP in pharmaceutical products utilizing GO/HA/GCE.

Sample	Added (μM)	Found (μM)	RSD (n = 3) (%)
Paracetamol 1	5	5.52	0.93
Paracetamol 2	5	5.15	1.94
Paracetamol 3	5	4.95	1.57

4. Conclusion

In this work, the GO/HA nanocomposite was synthesized via a co-precipitation method and employed for the fabrication of an electrochemical sensor for 4-aminophenol (4-AP) detection. The GO/HA-modified glassy carbon electrode exhibited enhanced electrocatalytic activity toward 4-AP, achieving a low detection limit of 0.14 nM over a wide linear concentration range of 0.1–340 μM with a correlation coefficient of $R_2 = 0.9974$. The sensor preparation is simple, rapid, and reproducible, and the fabricated electrode shows good selectivity toward 4-AP. These results demonstrate that the GO/HA nanocomposite is a suitable material for the low-cost electrochemical sensing of 4-aminophenol, benefiting from the catalytic activity of HA and the high surface area of GO.

Acknowledgments: The author N. Sudhan acknowledges the Post Graduate and Research Department of Chemistry, Thiagarajar College, Madurai for providing research facilities to carry out this work. The Author A.Asrar Ahamed express gratitude to the Principal and Management committee members, Jamal Mohammed College, Trichy, providing necessary facilities funded by DBT and DST-FIST sponsored Jamal Instrumentation Centre.

Availability of Data and Materials: Data materials are available upon request.

Funding: There is no external funding received in this research.

Author Contributions: AAA—Conceptualization, methodology, software, writing—original draft, data curation, validation, visualization, resources. NS—Software, formal analysis, investigation, visualization, resources, validation, writing—review and editing. VB—Conceptualization, supervision, validation, investigation, funding acquisition, visualization, writing—review and editing, project administration, resources, methodology, data curation. K-KS-J—Conceptualization, formal analysis, writing—review and editing, visualization. VRR—Data validation, review and writing. All authors read and approved the final manuscript. All authors have participated sufficiently in the work and agreed to be accountable for all aspects of the work.

Conflicts of Interest: The authors declare no conflict of interest.

References

1. Kringstad, K.P.; Lindstrom, K. Spent liquors from pulp bleaching. *Environmental Science and Technology* 1984, 18, 236A–248A. https://doi.org/10.1021/es00126a714
2. United States Environmental Protection Agency. U.S. Environmental Protection Agency. Available online: http://www.epa.gov (accessed on February 2010).
3. Pendela, M.; Dragovic, S.; Bockx, L.; et al. Development of a liquid chromatographic method for the determination of related substances and assay of d-cycloserine. *Journal of Pharmaceutical and Biomedical Analysis* 2008, 47, 807–811. https://doi.org/10.1016/j.jpba.2008.03.012
4. Yesilada, A.; Erdogan, H.; Ertan, M. Second derivative spectrophotometric determination of p-aminophenol in the presence of paracetamol. *Analytical Letters* 1991, 24, 129–138. https://doi.org/10.1080/00032719108052889

5. European Pharmacopoeial Convention. European Pharmacopoeia, 6th ed. Council of Europe: Strasbourg, France; 2007. pp. 49.
6. United States Pharmacopeial Convention. The United States Pharmacopoeia 27–NF (National Formulary). USP Convention: Rockville, MD, USA; 2004. pp. 2494.
7. Vichapong, J.; Sookserm, M.; Srijesdaruk, V.; et al. HPLC analysis of phenolic compounds and antioxidant activities in rice varieties. *LWT—Food Science and Technology* 2010, 43, 1325–1330. https://doi.org/10.1016/j.lwt.2010.05.007
8. Masawat, P.; Liawruangrath, S.; Vaneesorn, Y.; et al. Design and fabrication of a low-cost flow-through cell for acetaminophen determination by flow injection cyclic voltammetry. *Talanta* 2002, 58, 1221–1234. https://doi.org/10.1016/S0039-9140(02)00424-1
9. Monser, L.; Darghouth, F. Simultaneous LC determination of paracetamol and related compounds in pharmaceutical formulations using a carbon-based column. *Journal of Pharmaceutical and Biomedical Analysis* 2002, 27, 851–860. https://doi.org/10.1016/S0731-7085(01)00515-5
10. Kuila, T.; Bose, S.; Khanra, P.; et al. Recent advances in graphene-based biosensors. *Biosensors and Bioelectronics* 2011, 26, 4637–4648. https://doi.org/10.1016/j.bios.2011.05.039
11. Wang, X.; Zhi, L.J.; Müllen, K. Transparent, conductive graphene electrodes for dye -sensitized solar cells. *Nano Letters* 2008, 8, 323–327. https://doi.org/10.1021/nl072838r
12. Barbieri, O.; Hahn, M.; Herzog, A.; et al. Capacitance limits of high surface area activated carbons. *Carbon* 2005, 43, 1303–1310. https://doi.org/10.1016/j.carbon.2005.01.001
13. Kanchana, P.; Lavanya, N.; Sekar, C. Development of amperometric L-tyrosine sensor based on Fe -doped hydroxyapatite nanoparticles. *Materials Science and Engineering: C* 2014, 35, 85–91. https://doi.org/10.1016/j.msec.2013.10.013
14. Zanin, H.; Saito, E.; Marciano, F.R.; et al. Fast preparation of nano-hydroxyapatite/superhydrophilic reduced graphene oxide composites for bioactive applications. *Journal of Materials Chemistry B* 2013, 1, 4947–4955. https://doi.org/10.1039/C3TB20550A
15. Liu, Y.; Huang, J.; Li, H. Synthesis of hydroxyapatite–reduced graphite oxide nanocomposites via oriented nucleation and epitaxial growth of hydroxyapatite. *Journal of Materials Chemistry B* 2013, 1, 1826–1834. https://doi.org/10.1039/C3TB00531C
16. Gilje, S.; Han, S.; Wang, M.; et al. A chemical route to graphene for device applications. *Nano Letters* 2007, 7, 3394–3398. https://doi.org/10.1021/nl0717715
17. Fan, Z.J.; Wang, J.Q.; Wang, Z.F.; et al. One -pot synthesis of graphene/hydroxyapatite nanorod composite for tissue engineering. *Carbon* 2014, 66, 407–416. https://doi.org/10.1016/j.carbon.2013.09.016
18. Subrahmanyam, K.S.; Vivekchand, S.R.C.; Govindaraj, A.; et al. A study of graphenes prepared by different methods: characterization, properties and solubilization. *Journal of Materials Chemistry* 2008, 18, 1517–1523. https://doi.org/10.1039/B716536F
19. Yin, H.S.; Ma, Q.; Zhou, Y.L.; et al. Electrochemical behavior and voltammetric determination of 4-aminophenol based on graphene–chitosan composite film modified glassy carbon electrode. *Electrochimica Acta* 2010, 55, 7102–7108. https://doi.org/10.1016/j.electacta.2010.06.072
20. Fan, Y.; Liu, J.H.; Yang, C.P.; et al. Graphene–polyaniline composite film modified electrode for voltammetric determination of 4-aminophenol. *Sensors and Actuators B: Chemical* 2011, 157, 669–674. https://doi.org/10.1016/j.snb.2011.05.053
21. Shiroma, L.Y.; Santhiago, M.; Gobbi, A.L.; et al. Separation and electrochemical detection of paracetamol and 4-aminophenol on paper-based devices. *Analytica Chimica Acta* 2012, 725, 44–50. https://doi.org/10.1016/j.aca.2012.03.011
22. Zhang, X.; Wang, S.; Shen, Q. Electrocatalytic oxidation of 4-aminophenol at FeS_2/CNT-modified electrodes. *Microchimica Acta* 2005, 149, 37–42. https://doi.org/10.1007/s00604-004-0373-7
23. Huang, W.S.; Hu, W.B.; Song, J.C. Adsorptive stripping voltammetric determination of 4-aminophenol at a single-wall carbon nanotubes film coated electrode. *Talanta* 2003, 61, 411–416. https://doi.org/10.1016/S0039-9140(03)00302-3
24. Kelani, K.M.; Said, R.A.; El-Dosoky, M.A.; et al. Innovative voltammetric techniques for bumadizone analysis in pharmaceutical and biological samples: emphasizing green, white, and blue analytical approaches. *Scientific Reports* 2024, 14, 19873. https://doi.org/10.1038/s41598-024-69518-w

25. Kelani, K.M.; Abdel-Raoof, A.M.; Ashmawy, A.M.; et al. Electrochemical determination of dinitolmide in poultry product samples using a highly sensitive Mn2O3/MCNTs-NPs carbon paste electrode aided by greenness assessment tools. *Food Chemistry* 2022, 382, 131702. https://doi.org/10.1016/j.foodchem.2021.131702